

# ECMWF Feature article

.....  
from Newsletter Number 135 – Spring 2013

**METEOROLOGY**

.....  
The new MACC-II CO<sub>2</sub> forecast  
.....



[www.ecmwf.int/en/about/news-centre/media-resources](http://www.ecmwf.int/en/about/news-centre/media-resources)

doi:10.21957/ajm47w6h

This article appeared in the Meteorology section of ECMWF Newsletter No. 135 – Spring 2013, pp. 8–13.

## The new MACC-II CO<sub>2</sub> forecast

Anna Agustí-Panareda, Sebastien Massart, Souhail Boussetta,  
Gianpaolo Balsamo, Anton Beljaars, Frédéric Chevallier,  
Richard Engelen, Vincent-Henri Peuch, Miha Razinger

A new global atmospheric forecast of CO<sub>2</sub> is available as part of the pre-operational Monitoring of Atmospheric Composition and Climate – Interim Implementation (MACC-II) project. MACC II is funded by the European Community's Seventh Framework Programme and uses the infrastructure of ECMWF's Integrated Forecasting System (IFS). Monitoring and understanding the current CO<sub>2</sub> variability is a prerequisite for climate projection and climate change adaptation, since it is the most abundant greenhouse gas with a large human-induced contribution.

In this article we present one of the first operational CO<sub>2</sub> forecast products that is available in real time. This is important because it opens up the possibility of assimilating CO<sub>2</sub> observations in the IFS. It also allows the full interaction of the modelling of vegetation (via biogenic CO<sub>2</sub> fluxes), water cycle (via evapotranspiration) and radiation (via atmospheric CO<sub>2</sub>) within the ECMWF modelling framework.

First, we discuss the causes of CO<sub>2</sub> variability and describe the configuration of the forecast. Then we show the capability of the forecast to simulate CO<sub>2</sub> variability on different spatial and temporal scales by comparing forecasts with observations. The main sources of forecast error are pointed out as well as planned future work to address those issues. Finally, information on how to access the near-real-time CO<sub>2</sub> plots and the monitoring of the forecast, as well as the forecast data, is provided for anybody interested in using the CO<sub>2</sub> forecast product. Some of the potential applications of the CO<sub>2</sub> forecast are listed in Box A.

### Applications for the CO<sub>2</sub> forecast

A

The target applications of the MACC-II global CO<sub>2</sub> product include:

- Providing boundary conditions for regional modelling and flux inversions.
- Improving the modelling of the radiative transfer and evapotranspiration in Numerical Weather Prediction (NWP) analysis and forecast.
- Evaluation of transport processes in the IFS (e.g. diffusion, convection and advection).
- Providing prior information for CO<sub>2</sub> and CH<sub>4</sub> satellite retrievals.
- Supporting the interpretation and quality control of observations via monitoring activities.
- Supporting the planning of field experiments.

### CO<sub>2</sub> variability

The variability of atmospheric CO<sub>2</sub> concentration results from variations in surface fluxes and atmospheric transport, which are coupled. The challenge of forecasting CO<sub>2</sub> globally arises from the large uncertainties in the simulation of the CO<sub>2</sub> sources and sinks and of atmospheric transport (particularly within the atmospheric boundary layer).

Globally, CO<sub>2</sub> variability on time scales ranging from diurnal, through seasonal to inter-annual is dominated by variations in the vegetation fluxes over land. The photosynthesis in plants and the respiration in both plants and organic soils result in large amounts of CO<sub>2</sub> being removed from and released into the atmosphere. These two processes vary with temperature, availability of moisture and radiation; hence producing daily, seasonal, annual and latitudinal variations in atmospheric CO<sub>2</sub> concentrations.

The recent development of the CTESSEL simplified land carbon module (Boussetta et al., 2013) used in the IFS provides terrestrial biogenic CO<sub>2</sub> fluxes in real time with accurate real-time meteorological forcing. It also ensures consistency between meteorological forcing of CO<sub>2</sub> biogenic fluxes and CO<sub>2</sub> transport.

An example of the importance of this consistency between forcing and transport is the passage of mid-latitude frontal weather systems. The change in radiation associated with the frontal clouds reduces photosynthetic CO<sub>2</sub> uptake which results in a substantial increase in atmospheric CO<sub>2</sub>, of the order of 10 ppm. This CO<sub>2</sub> concentration anomaly is then transported by frontal ascent to the mid- and upper-troposphere.

The coupling between fluxes and transport also works on seasonal scales. Namely, meridional transport by mid-latitude weather systems reduces/amplifies the CO<sub>2</sub> seasonal cycle at mid/high latitudes (Parazoo et al., 2011). On both diurnal and seasonal time scales, there is also a strong coupling between turbulent mixing near the ground and terrestrial biogenic fluxes, known as the rectifier effect (Denning et al., 1999).

### Forecast configuration

The CO<sub>2</sub> surface fluxes representing the various CO<sub>2</sub> sources and sinks in the CO<sub>2</sub> forecast are described in Box B. At present, the CO<sub>2</sub> forecast runs daily in a cyclic mode. That is, the atmospheric CO<sub>2</sub> is initialized each day at 00 UTC with the previous 24-hour forecast; this is in contrast with the NWP framework, where initial conditions are constrained by observations. In order to avoid growing CO<sub>2</sub> biases, the atmospheric CO<sub>2</sub> field is re-initialized on 1 January from simulations with the latest available optimized fluxes provided by the MACC-II flux inversion system at Laboratoire des Sciences du Climat et l'Environnement (LSCE, Chevallier et al., 2011). The meteorological fields are initialized with ECMWF operational analyses each forecast cycle.

The resolution of the CO<sub>2</sub> forecast is the same as the operational weather forecast. Currently, it has a lead time of 5 days with fields archived every 3 hours. This can be easily extended to longer lead times for specific user requirements.

#### CO<sub>2</sub> surface fluxes

**B**

The following outlines the CO<sub>2</sub> surface fluxes that represent the various CO<sub>2</sub> sources and sinks in the CO<sub>2</sub> forecast.

- CTESSEL includes a light-efficiency photosynthesis model driven by radiation, soil moisture and soil temperature. It has a simple parametrization for respiration driven by soil moisture, soil temperature and snow cover. The vegetation growth is derived from a MODIS-based LAI climatology and land use change is not represented. There is no direct simulation of the different carbon pools, but a reference respiration parameter for each vegetation type is used to simulate the ecosystem respiration. The reference value is obtained by optimization with respect to flux measurements for the different vegetation types. A detailed description and evaluation of the CTESSEL biogenic fluxes has been provided by (Boussetta et al., 2013, *ECMWF Tech. Memo. No. 675*).
- The near-real-time fire flux is from GFAS v1.0 Kaiser et al., 2012, *Biogeosciences*, **9**, 527–554  
• [http://www.gmes-atmosphere.eu/about/project\\_structure/input\\_data/d\\_fire/](http://www.gmes-atmosphere.eu/about/project_structure/input_data/d_fire/) a daily temporal resolution and a horizontal resolution of 0.5° × 0.5°. The fire fluxes are kept constant throughout the 5-day forecast.
- The ocean sink is from the Takahashi et al. (2009, *Deep-Sea Res. II*, **56**, 554–577) climatology with monthly mean fluxes at 4° × 5° resolution.
- The anthropogenic fluxes are annual mean fluxes based on the last year (2008) of the EDGAR version 4.2 inventory  
• <http://edgar.jrc.ec.europa.eu> in order to account for the increase in the emissions since 2008, the growth in anthropogenic emissions beyond 2008 has been represented using a global rescaling factor based on estimated and climatological anthropogenic CO<sub>2</sub> emission trends.

### Annual global budget

The increase of atmospheric CO<sub>2</sub> concentration in the model is the result of the addition of all the CO<sub>2</sub> surface fluxes shown in Figure 1. Because the CO<sub>2</sub> fluxes in the model are not constrained by observations, the sum of the total emissions (i.e. the budget) does not match the observed atmospheric increase. This leads to an annual global bias in the forecast of CO<sub>2</sub>. This bias and the modelled atmospheric concentration increase are both modulated by the inter-annual variability of the terrestrial biogenic fluxes. The correlation between the forecast and observed global annual atmospheric growth is 0.74. Although the main contributor to the CO<sub>2</sub> sink associated with the terrestrial biogenic fluxes is the northern hemisphere, the tropics are responsible for its large inter-annual variability.

### Seasonal cycle

The phase and amplitude of the CO<sub>2</sub> seasonal cycle vary with latitude. The model is evaluated using the NOAA GLOBALVIEW-CO<sub>2</sub> (2011) dataset which provides the integrated effects of surface CO<sub>2</sub> fluxes over large regions at different latitudinal bands.

At first glance, the seasonal cycle phase and amplitude and latitude dependence shown in Figure 2 appear to be reasonably well represented in the forecast. However, there are clear discrepancies between the forecast and GLOBALVIEW-CO<sub>2</sub> product in the northern hemisphere.

- In the forecast not enough CO<sub>2</sub> is released before and after the growing season (i.e. March to May and October to December).
- The onset of the CO<sub>2</sub> sink associated with the growing season starts too early in the forecast (e.g. the sharp CO<sub>2</sub> decrease in mid-latitudes depicted by GLOBALVIEW-CO<sub>2</sub> product in June starts in May in the forecast). This also leads to a longer growing season in the forecast.

The combination of these two factors is consistent with the predominantly negative global annual bias shown in Figure 1.

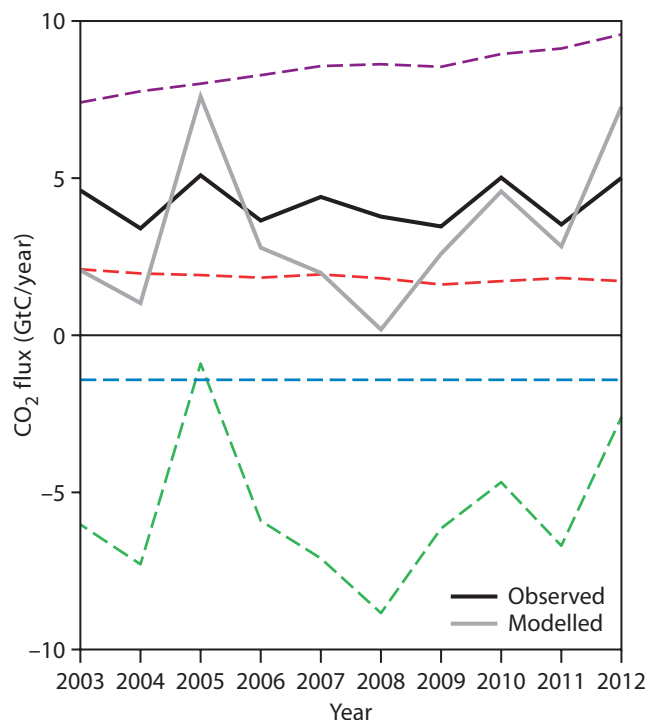


**Figure 1** Annual global budget for the modelled total CO<sub>2</sub> flux (grey) compared to the observed CO<sub>2</sub> atmospheric growth from NOAA (<http://www.esrl.noaa.gov/gmd/ccgg/trends/>) (black) from 2003 to 2012. The different flux components are shown by the other coloured lines: anthropogenic (purple), fires (red), ocean (blue) and land vegetation (green). The units are gigatons of carbon (GtC).

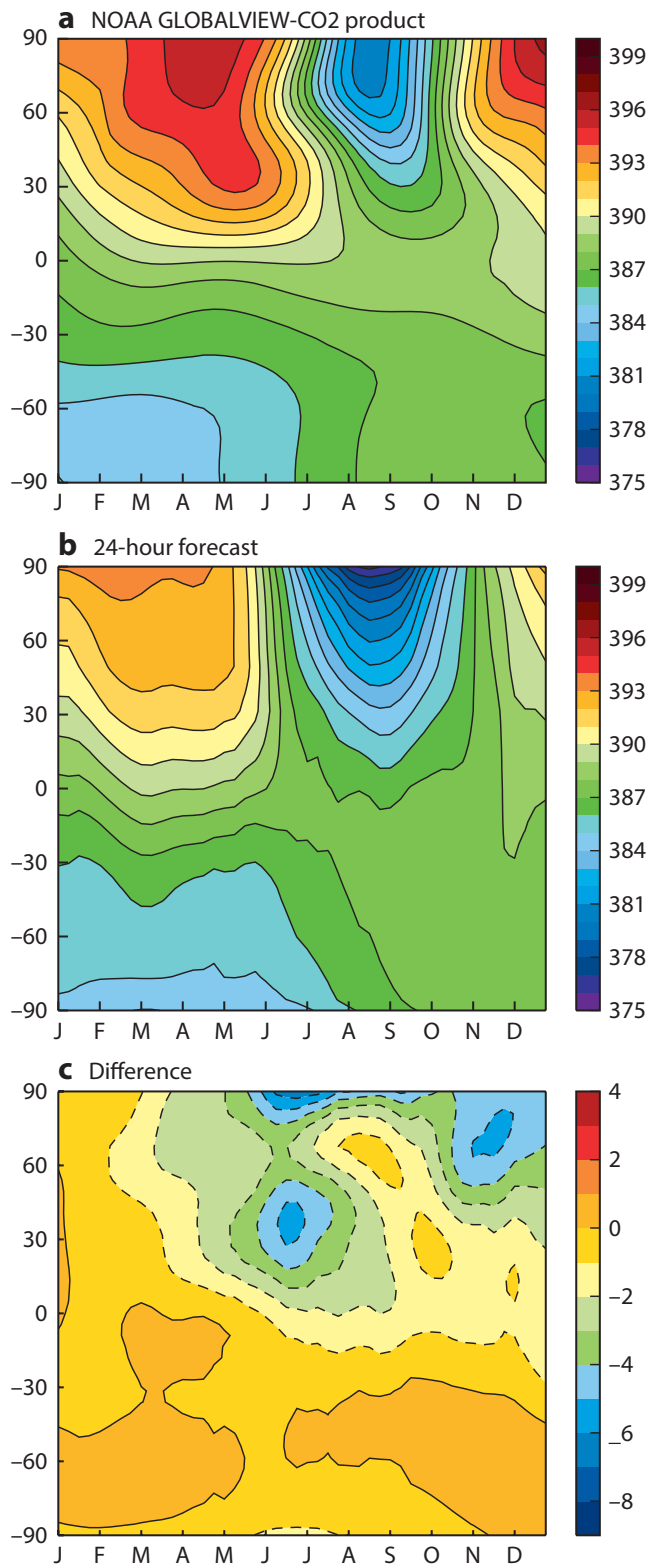


**Figure 2** (a) NOAA GLOBALVIEW-CO<sub>2</sub> product for 2010 based on observations, (b) the equivalent product based on the 24-hour forecast of CO<sub>2</sub>, and (c) the difference between the GLOBALVIEW product and the forecast. The CO<sub>2</sub> forecast has been sampled at the same locations as the GLOBALVIEW observations and the same data processing described in Masarie & Tans (1995, *J. Geophys. Res.*, 100, No. D6, 11593–11610) has been applied. Thanks to NOAA/ESRL for providing the GLOBALVIEW-CO<sub>2</sub> product.

### Synoptic variability

The passage of frontal low pressure systems is responsible for the long-range transport of CO<sub>2</sub> via their warm conveyor belts which lift CO<sub>2</sub>-rich air from the surface to the mid- and upper-troposphere. This large-scale advection is illustrated in Figure 3a where positive CO<sub>2</sub> anomalies originating from the surface are shown in the region of frontal ascent within a low pressure system at various vertical levels (850, 500 and 300 hPa).

The synoptic variability of CO<sub>2</sub> associated with the passage of low pressure systems is well captured by the forecast at the NOAA/ESRL tall tower in Park Falls (Wisconsin, USA), as shown in Figures 3b and 3c throughout September. The high peaks of CO<sub>2</sub> concentration can originate from the advection of CO<sub>2</sub>-rich anomalies, as well as the synoptic variability of the CO<sub>2</sub> net ecosystem exchange fluxes.

The cloudy warm conveyor belts in the mid-latitude low pressure systems are associated with changes in temperature and solar radiation at the surface which in turn produce an increase in the net ecosystem exchange. As shown in Figure 4, this increase can be linked with the following.

- A decrease in the photosynthetic uptake following a decrease in radiation (e.g. 3 and 7 September) – see panels 4a and 4c.
- An increase in ecosystem respiration following an increase in temperature (e.g. 21 September) – see panels 4a and 4b.
- Both, a simultaneous decrease in the vegetation uptake and increase in ecosystem respiration due to a concurrent decrease in radiation and increase in temperature (e.g. 11 and 23 to 24 September) – see panels 4a, 4b and 4c.

The landfall of hurricane Sandy in 2012 provides another example of the importance of the passage of low-pressure systems in the modulation of CO<sub>2</sub> synoptic variability and long-range transport. The various CO<sub>2</sub> anomalies shown in Figure 5 are associated with convective, synoptic and large-scale transport mechanisms. Thus, the CO<sub>2</sub> forecast opens the possibility of using CO<sub>2</sub> as a tracer to provide information about the transport processes in NWP models.

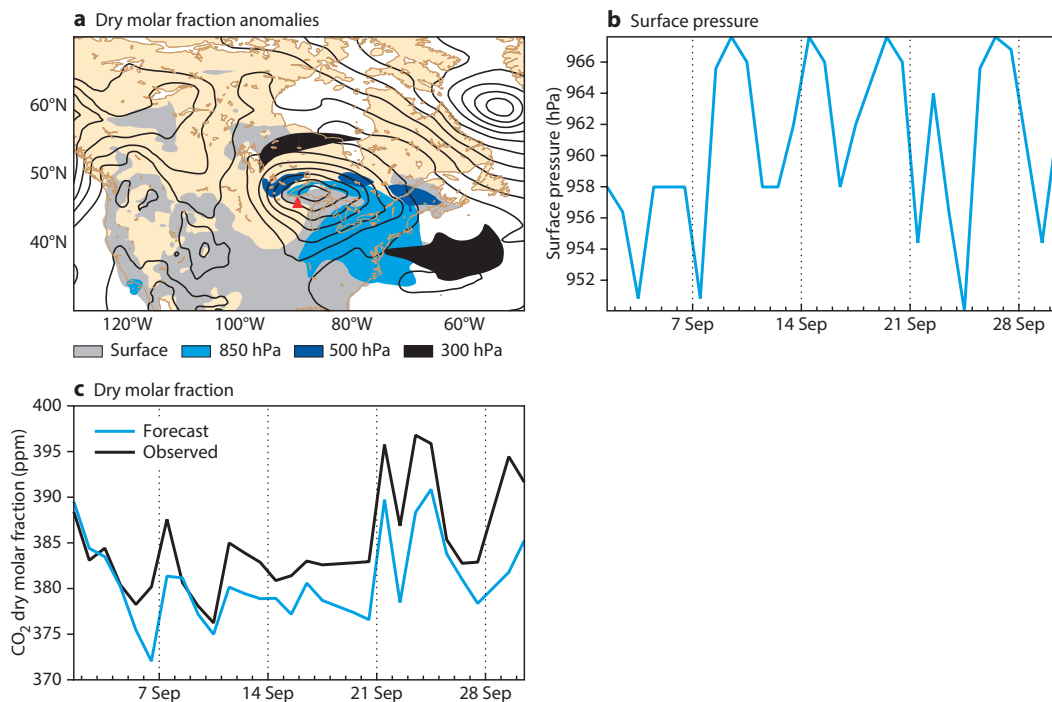


**Figure 3** (a) CO<sub>2</sub> dry molar fraction anomalies [ppm]. Areas above a threshold of 392 ppm at the 10-metre level are shaded in grey, areas above 392 ppm at the 850 hPa level are shaded in cyan, areas above 388 ppm at the 500 hPa level are shaded in blue and areas above 388 ppm at the 300 hPa level are shaded in black. Contours depict mean sea level pressure. The location of Park Falls is depicted by a red triangle. (b) ECMWF surface pressure forecast [hPa] and (c) daily mean CO<sub>2</sub> dry molar fraction [ppm] from the 24-hour forecasts in cyan and observed CO<sub>2</sub> in black at Park Falls in September 2010. Thanks to Arlene Andrews (NOAA/ESRL) for providing the CO<sub>2</sub> observations from the top level (396 m) of the ESRL/NOAA tall tower (Andrews et al., 2013, *Atmos. Meas. Tech. Discuss.*, 6, 1461–1553) at Park Falls (45.95°N, 90.27°W, 472 m a.s.l, Wisconsin, USA).



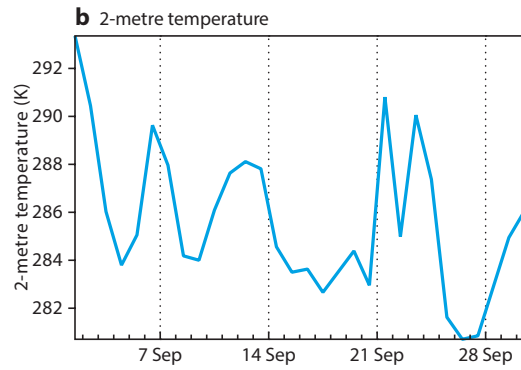
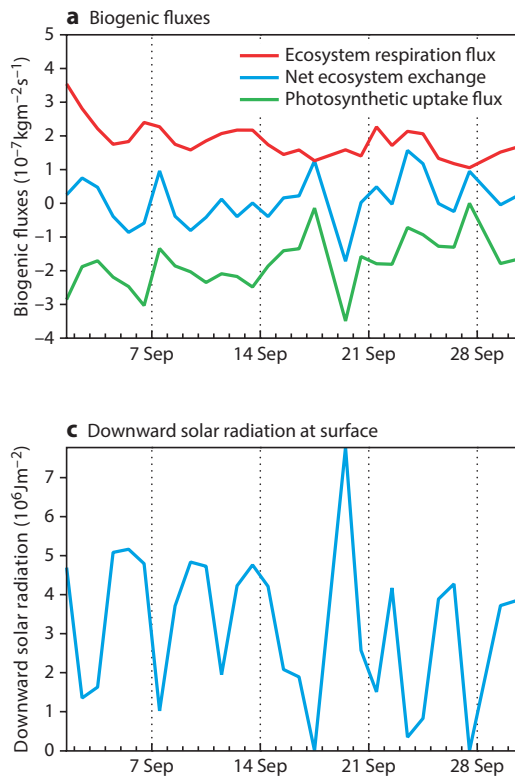


**Figure 4** (a) Daily mean biogenic fluxes: net ecosystem exchange in cyan, photosynthetic uptake fluxes in green and ecosystem respiration fluxes in red [ $\text{kg m}^{-2} \text{ s}^{-1}$ ], (b) daily mean 2-metre temperature [K] and (c) daily mean downward solar radiation at the surface [ $\text{J m}^{-2}$ ] from the 24-hour forecast at Park Falls in September 2010.

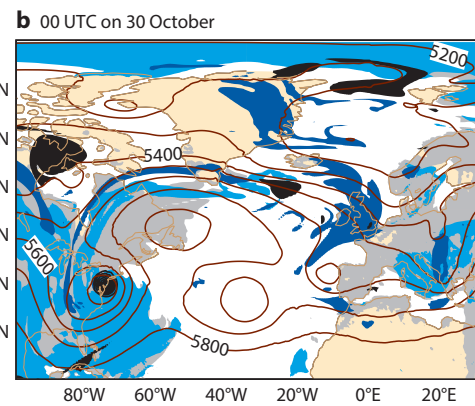
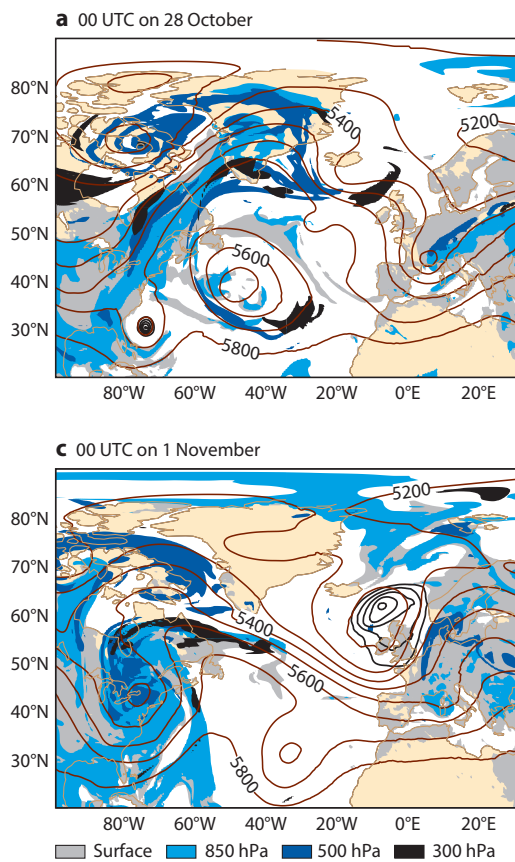


**Figure 5** CO<sub>2</sub> dry molar fraction anomalies [ppm] depicting the landfall of Hurricane Sandy on (a) 28 October, (b) 30 October and (c) 1 November 2012. Areas above a threshold of 392 ppm are shaded in grey for the 10-metre level, in cyan for the 850 hPa level, in blue for the 500 hPa level and in black for the 300 hPa level. Brown and black contours depict geopotential height at 500 hPa and mean sea level pressure below 980 hPa respectively.

## Diurnal cycle

Over vegetated areas, CO<sub>2</sub> concentration is characterized by a strong diurnal cycle controlled by the CO<sub>2</sub> biogenic fluxes – day-time uptake and night time release – as well as the boundary layer increased/decreased mixing during daytime/night time.

Figure 6 shows the diurnal cycle in the CO<sub>2</sub> forecast and observations at the ICOS (Integrated Carbon Observation System) tower at Cabauw in The Netherlands in June 2012. In the forecast, the day-time low-CO<sub>2</sub> values are consistently underestimated at all sampling levels; whereas at night-time, the forecast errors are not consistent at all sampling heights. This can be explained by the decoupling between lower and upper sampling heights during night-time stable conditions when the boundary layer collapses. Close to the surface, the night-time atmospheric CO<sub>2</sub> peak is also much more variable than the day-time CO<sub>2</sub>. This large atmospheric CO<sub>2</sub> variability at night-time is associated with a strong coupling between the night-time CO<sub>2</sub> emissions and the decrease in the boundary layer height. Therefore, the CO<sub>2</sub> forecast can also be useful as an extra diagnostic in assessing the boundary layer turbulent mixing in the IFS, particularly in stable night-time conditions.

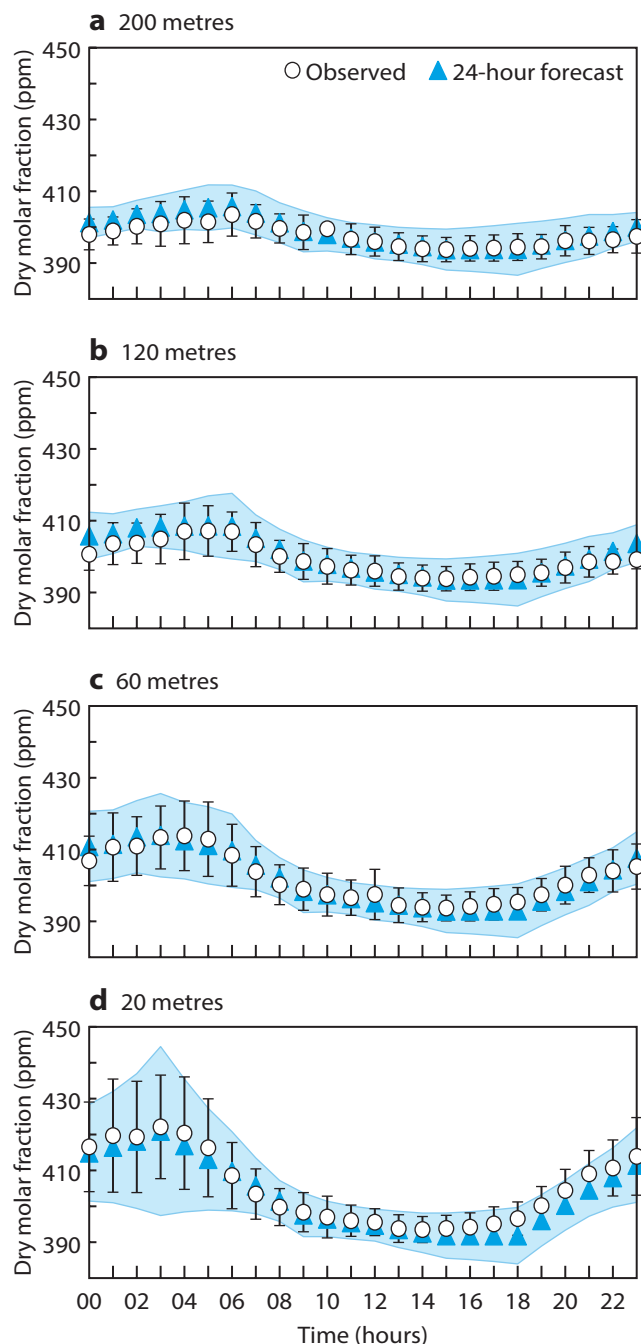


**Figure 6** Mean diurnal cycle of CO<sub>2</sub> dry molar fraction [ppm] at four levels at the ICOS tall tower at Cabauw (51.97°N, 4.93°E, Netherlands) from measurements (circles) and 24-hour forecast (blue triangles) in June 2012. The standard deviations of observation and forecast day-to-day variability are shown as black bars and blue shading respectively. Thanks to Jérôme Tarniewicz (ICOS Atmospheric Thematic Center), and Philippe Ciais and Michel Ramonet (Laboratoire des Sciences du Climat et l'Environnement) for providing the data for MACC-II from the website at <https://icos-atc-demo.lsce.ipsl.fr>, as well as Alex Vermeulen (Energy research Centre of the Netherlands, ECN), the Principal Investigator from Cabauw station. The authors acknowledge the European Commission for the support of the preparatory phase of ICOS (2008–2013) and the Netherlands Ministry of Infrastructure and the Environment and ECN for the support of the observations at Cabauw.



### Uncertainties and future developments

As the CO<sub>2</sub> forecast is not constrained by CO<sub>2</sub> observations, it is globally biased. The offset is largest in the northern hemisphere and is associated predominantly with errors in the land vegetation fluxes in northern hemisphere mid-latitudes, particularly during the growing season. Despite the biases, overall the forecast simulates well the CO<sub>2</sub> synoptic variability modulated by the coupling between meteorological forcing of the fluxes and transport. Even during the spring months, when the synoptic variability in the model does not correlate well with the observed variability, there are significant correlations between meteorological parameters and observed CO<sub>2</sub>. This implies that there is scope to improve the model. These model uncertainties will be addressed in the near future as part of the ongoing efforts to upgrade the real-time CO<sub>2</sub> forecasting system of the future Copernicus atmospheric service.

### Data access and near-real-time monitoring

The CO<sub>2</sub> observations provided in near real time by the operational ICOS network are invaluable for the monitoring of the CO<sub>2</sub> forecast. Continuous near-real-time monitoring of the MACC-II CO<sub>2</sub> forecast based on the pre-operational ICOS network is available online.

- <http://www.gmes-atmosphere.eu/d/services/gac/verif/ghg/icos/>

This evaluation supports the ongoing assessment of the model errors. It is also the first step towards assimilating in situ CO<sub>2</sub> observations into the forecasting system. In return, the daily CO<sub>2</sub> forecasts prove very valuable for the ICOS data providers by allowing a better large-scale interpretation of the time series at the various observation locations.

Global maps of the 5-day forecast, run every day from 00 UTC, can be accessed online

- [http://www.gmes-atmosphere.eu/d/services/gac/nrt/nrt\\_fields\\_co2/](http://www.gmes-atmosphere.eu/d/services/gac/nrt/nrt_fields_co2/)

The real-time global CO<sub>2</sub> forecast data is also available in the MACC-II data catalogue

- <http://www.gmes-atmosphere.eu/catalogue/>

We have seen that despite the biases associated mainly with the biogenic flux errors, the CO<sub>2</sub> forecast has skill in representing variability at synoptic scales. We are currently exploring the assimilation of CO<sub>2</sub> in situ and satellite retrievals in the IFS. However, in order to deliver a CO<sub>2</sub> analysis product in near real time, it is crucial that as many CO<sub>2</sub> observations and retrievals as possible are provided in near real time.

As well as the forecast of CO<sub>2</sub> supporting a variety of applications, we hope it will also be useful for regional modelling of CO<sub>2</sub> and future NWP developments. These include the evaluation of boundary layer mixing, the coupling of CO<sub>2</sub> with radiation in the NWP forecast and analysis, and the modelling of evapotranspiration.

### Further reading

**Boussetta, S., G. Balsamo, A. Beljaars, A. Agustí-Panareda, J.-C. Calvet, C. Jacobs, B. van den Hurk, P. Viterbo, S. Lafont, E. Dutra, L. Jarlan, M. Balzarolo, D. Papale & G. van der Werf**, 2013: Natural carbon dioxide exchanges in the ECMWF Integrated Forecasting System: Implementation and offline validation. *ECMWF Tech. Memo. No. 675*.

**Chevallier, F., P. Ciais, T.J. Conway, T. Aalto, B.E. Anderson, P. Bousquet, E.G. Brunke, L. Ciattaglia, Y. Esaki, M. Fröhlich, A. Gomez, A.J. Gomez-Pelaez, L. Haszpra, P.B. Krummel, R.L. Langenfelds, M. Leuenberger, T. Machida, F. Maignan, H. Matsueda, J.A. Morguí, H. Mukai, T. Nakazawa, P. Peylin, M. Ramonet, L. Rivier, Y. Sawa, M. Schmidt, L.P. Steele, S.A. Vay, A.T. Vermeulen, S. Wofsy & D. Worthy**, 2011: CO<sub>2</sub> surface fluxes at grid point scale estimated from a global 21-year reanalysis of atmospheric measurements, 2010: *J. Geophys. Res.*, **115**, D21307, doi:10.1029/2010JD013887.

**Denning, A.S., T. Takahashi & P. Friedlingstein**, 1999: Can a strong atmospheric CO<sub>2</sub> rectifier effect be reconciled with a “reasonable” carbon budget?, *Tellus*, **51B**, 249–253.

**GLOBALVIEW-CO<sub>2</sub>**, 2011: Cooperative Atmospheric Data Integration Project – Carbon Dioxide. NOAA ESRL, Boulder, Colorado (Available at <http://www.esrl.noaa.gov/gmd/ccgg/globalview/>).

**Parazoo, N.C., A.S. Denning, J.A. Berry, A. Wolf, A.D. Randall, S.R. Kawa, O. Pauluis & S.C. Doney**, 2011: Moist synoptic transport of CO<sub>2</sub> along the mid-latitude storm track, *Geophys. Res. Lett.*, **38**, L09804, doi:10.1029/2011GL047238.

© Copyright 2016

European Centre for Medium-Range Weather Forecasts, Shinfield Park, Reading, RG2 9AX, England

The content of this Newsletter article is available for use under a Creative Commons Attribution-Non-Commercial-No-Derivatives-4.0-Unported Licence. See the terms at <https://creativecommons.org/licenses/by-nc-nd/4.0/>.

The information within this publication is given in good faith and considered to be true, but ECMWF accepts no liability for error or omission or for loss or damage arising from its use.